

Tribocorrosion behaviour of plasma nitrided and plasma nitrided + oxidised Ti6Al4V alloy

A.C. Fernandes ^{a,*}, F. Vaz ^a, E. Ariza ^b, L.A. Rocha ^b, A.R.L. Ribeiro ^b,
A.C. Vieira ^b, J.P. Rivière ^c, L. Pichon ^c

^a Universidade do Minho, Dept. Física, Campus de Azurém, 4800-058 Guimarães, Portugal

^b Universidade do Minho, Dept. Eng. Mecânica, Azurém, 4800-058 Guimarães, Portugal

^c Laboratoire de Métallurgie Physique, Université de Poitiers, 86960 Futuroscope, France

Available online 20 December 2005

Abstract

This paper reports the influence of low pressure plasma nitriding treatments, some of them followed by plasma assisted oxidation on the mechanical properties and tribocorrosion resistance of a Ti6Al4V alloy. Nitridation was performed for 640 or 720 min at 600 and 700 °C in a r.f. plasma equipment, using a N₂–H₂ gas mixture at 7.5 Pa. Some of the samples were then post-oxidized at 700 °C for 15 and 60 min, within a O₂ plasma of 9.5 Pa. XRD results revealed the occurrence of the Ti₂N phase for the nitrided samples. The oxidized surface layers are poorly crystallised with rutile and traces of anatase TiO₂ nanocrystallites. Microhardness tests showed a significant improvement of the surface hardness whatever the treatment, with a slight effect of the treatment temperature. The tribocorrosion results clearly showed that plasma treatments have a strong influence on the tribocorrosion behaviour of the material. Both the corrosion and wear performance of the samples are improved by the increase of the processing temperature.

© 2005 Elsevier B.V. All rights reserved.

Keywords: Titanium; Pin-on-disc; X-ray diffraction; Plasma treatment

1. Introduction

Ti6Al4V (wt.%) is one of the most used titanium alloys due to its lower density than pure titanium, but with more favourable physical and mechanical properties. Those properties make it of particular interest in biomaterials and aeronautic applications [1–5]. This material has a two-phase structure: a hexagonal α -Ti phase with aluminium in solid solution and a β -Ti phase with vanadium stabilised cubic lattice [6]. This biphasic structure contributes to a higher mechanical strength compared to pure Ti [6]. However, the use of this alloy in everyday life applications is still very limited due to its poor wear resistance [2,4,7,8]. In case of oxidant or corrosive atmospheres, the degradation is even worse, leading to the inevitable replacement of the working pieces. Thus, surface treatments such as nitridation or oxidation are being investigated as possible solutions to improve the surface properties of this alloy [4,9–12]. Acting as a diffusion barrier, the nitride layer and the underneath

gradient relate a decrease of solubility and also the diffusivity of nitrogen compared to the pure alloy, and thus preventing further oxygen dissolutions deeper into the alloy [10].

Taking this into consideration, the main purpose of this work was to carry out protective oxygen and nitrogen plasma treatments on Ti6Al4V samples, in an original apparatus previously described [13]. The temperature and the duration of the treatments were the studied parameters. These treatments modified the surface structure by the formation of different crystalline phases such as TiO₂, Ti₂N, TiN and α -Ti(N,O) (solid solution of nitrogen and oxygen in titanium) [5,14]. The presence of these crystalline phases results in hardness enhancement of the material [15], and may consequently increase its wear and the corrosion resistance properties in many aggressive environments [7].

2. Experimental

The surface treatment reactor chamber is composed of a quartz tube surrounded by a tubular furnace, allowing the temperature control from room temperature up to 1000 °C [13].

* Corresponding author. Tel.: +351 253 510475; fax: +351 253 510461.

E-mail address: acrist@fisica.uminho.pt (A.C. Fernandes).

The base pressure in the chamber was about 10^{-5} Pa. Two samples, A and B, were nitrided for 14 h at 600 °C and 12 h at 700 °C, respectively, in a 7.5 Pa atmosphere. A N_2-H_2 (50%–50%) gas mixture was used. The gas reactivity was activated by a radio-frequency (r.f.) electromagnetic excitation (forward power: 700 W), resulting in the creation of a cold plasma (ion density about 10^9 ions/cm³). In order to study the influence of oxidation, samples B-ox1 and B-ox2 were oxidised at 700 °C with r.f. plasma (700 W) for 15 to 60 min, respectively, in a 9.5 Pa pure oxygen atmosphere, after the 700 °C nitridation process (12 h). The oxidation of sample B-ox1 was carried out after the nitridation without cooling the sample. Sample B-ox2 was cooled after the nitridation to room temperature, and then heated again for the oxidation. For comparison purposes, a solely oxidised sample, ox2, was also prepared at 700 °C for 1 h. The thermal cycle of the nitriding was carried out by heating the samples up to 50 °C below the desired temperature at a rate of 20 °C/min. The last 50 °C was carried out at a rate of 20 °C/min.

Chemical depth profiles were obtained by Glow Discharge Optical Emission Spectroscopy (GDOES), on a Jobyn-Yvon RF-GD Profiler. Structure was investigated by X-ray diffraction (XRD), using a Siemens D5005 diffractometer (Cu $K\alpha$ monochromatic radiation). Microhardness was measured on a SHIMADZU HMV 2000 apparatus, equipped with a Vickers indenter. The measurements were performed on the sample surface and cross-sections (using a “sandwich” of two samples with treated faces glowed together), using 100 and 25 g during 15 s, respectively.

Wear-corrosion experiments were carried out in a pin-on-plate tribometer (Plint TE67/R) with an alumina pin. The contact was immersed in a 0.9 wt.% NaCl electrolyte and all

open-circuit potentials (OCP) were measured and expressed with reference to a saturated calomel electrode (SCE), and a platinum wire with an area of 1 cm² was used as counter electrode. The displacement amplitude was 3 mm and the normal load was fixed at 3 N. Electrochemical Impedance Spectroscopy (EIS) measurements were performed before and after the sliding at open-circuit potential in the frequency range of 100 kHz to 10 mHz, applying an ac current with an amplitude of 10 mV. The area of the working electrode was set at 0.64 cm². A PGP201 Potentiostat/Galvanostat (Radiometer Analytical, Denmark), controlled by the VoltaMaster software, was used to carry out the polarization measurements, while a Voltalab PGZ100 Potentiostat (Radiometer Analytical, Denmark), controlled by the VoltaMaster-4 software, was used for the EIS measurements.

3. Results

3.1. Surface composition

Results of chemical profiles obtained by GDOES are shown in Fig. 1, illustrating 4 of the analyzed samples. On the top surface of all samples, a pollution and native oxide layer of few nanometers was found. Below this layer, the nitrided samples revealed a nitride layer of about 0.25 μ m at 600 °C and 0.7 μ m at 700 °C, and close to an average Ti_2N stoichiometry. These results are in agreement with the literature data and the N diffusion coefficient in Ti, Ti_2N and TiN [16].

Regarding the Ti6Al4V sample oxidized for 1 h (Ox2), an oxide layer of about 0.5 μ m can be observed. The oxygen composition of the whole oxide layer (~55 at.%) is slightly

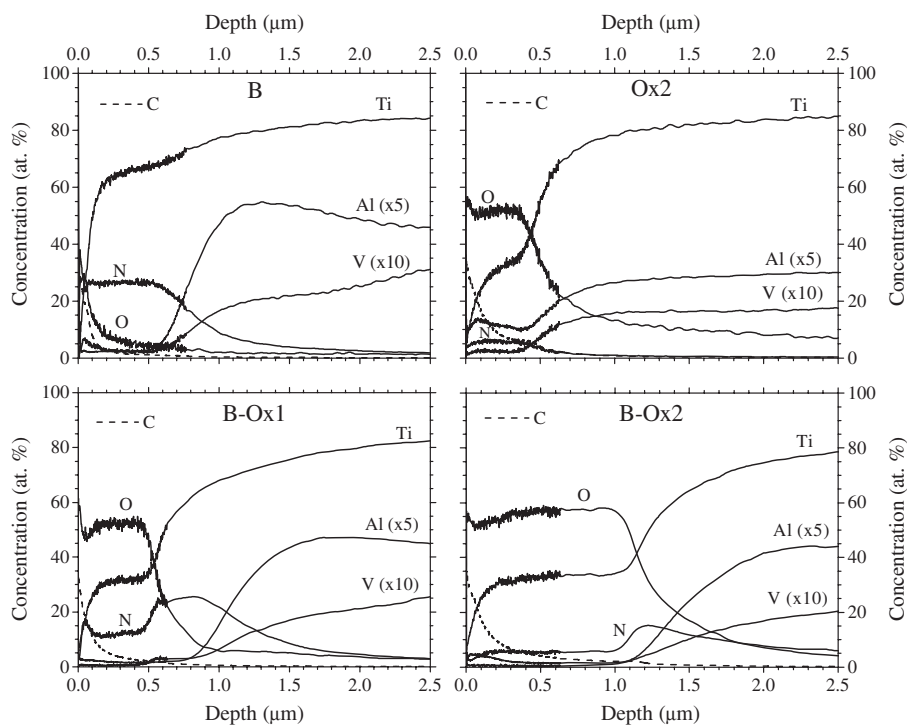


Fig. 1. Element profiles obtained by GDOES for B, Ox2, B-Ox1 and B-Ox2 samples. The results obtained for Al and V are multiplied by 5 and 10, respectively.

understoichiometric compared to the expected one in TiO_2 (67 at.%). The relative stoichiometry between the metallic elements Ti, Al and V remains almost unmodified compared to the initial alloy, except at the top surface, within the first 100 nm which is an aluminium rich zone (possibly in the form of an oxide). These observations are consistent with the literature on the first steps of the oxidation mechanism of Ti6Al4V [17].

After their oxidation, the pre-nitrided samples (B-ox1 and B-ox2) are composed of a surface oxide layer ~ 55 at.% O and some remaining N (~ 5 at.%). This surface layer is followed by an interface zone with a decreasing O concentration, but a higher N concentration (15 at.%) which can be seen as a remaining part of the previous nitride layer. Finally, there is a long range diffusion depth with gradients of O and N on several microns. After 1 h of oxidation, the surface oxide layer thickness is about 1 μm (sample pre-nitrided at 700 °C) and 0.5 μm (sample pre-nitrided at 600 °C). Compared to the nitride layer thickness before oxidation, these values are in good agreement with the Pilling–Bedworth ratio expected between the Ti_2N and TiO_2 materials (1 μm of Ti_2N gives rise to about 1.67 μm of TiO_2). The oxide layer is more likely to be obtained by the more or less complete oxidation of the nitride, as shown by the remaining depletion in alloying elements Al and V.

3.2. Structure analysis

Fig. 2 shows the XRD diffraction patterns for all analyzed samples. The diffraction patterns corresponding to untreated sample (non-indexed in the diffractograms) correspond to the hexagonal α -Ti (JCPDS file 44-1294) and body centered cubic β -Ti (JCPDS file 44-1288) peaks. A slight angular shift is observed, which is probably due to dissolution of alloying elements of the alloy within the α -Ti (Al mainly) and the β -Ti (mainly V), resulting in the formation of a solid solution and compressive stresses [4]. Same behaviour seems also to occur after the treatments, especially those at the highest temperature, caused again by the incorporation of other elements (N and O) [10], noted in the figures as α -Ti(N,O).

In the nitrided samples (A and B, Fig. 2a) the main crystalline phase developed is the tetragonal ϵ - Ti_2N (JCPDS file 17-0386), which in fact correlates well with the composition analysis. Traces of cubic titanium nitride δ -TiN (JCPDS file 38-1420) nanocrystals might also be present, but just at the highest nitridation temperature. A slight shift in the ϵ - Ti_2N , of about 0.10° , seems to occur at 700 °C, which might be due to stresses generated by the large thickness of nitride [4]. The oxidised sample (Ox2, Fig. 2b) revealed a slight shift in some of the α -Ti peaks (or even a sum of different peaks, particularly visible in the region $40^\circ < 2\theta < 41^\circ$) towards lower diffraction angles, which might be the result of oxygen incorporation in this phase. Beyond this doped α -Ti phase, few traces of rutile and anatase-type TiO_2 can also be evidenced for this sample. The relatively low temperature and the short duration of the oxidation probably explain the few evidences for TiO_2 formation.

Regarding the nitrided+oxidised samples (B-ox1 and B-ox2), the main result is the enhancement of rutile phase, especially in the sample treated for longer oxidation time (B-

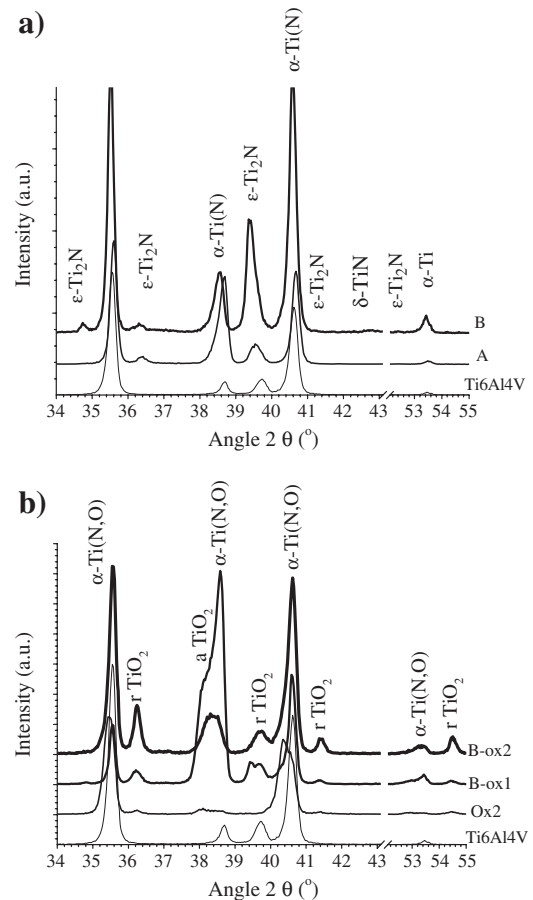


Fig. 2. XRD diffractograms of samples (a) nitrided and (b) nitrided+oxidised and oxidised.

ox2). This result has to be compared to the composition analysis that revealed different repartitions of aluminium. Again, the shift of α -Ti peaks is clearly visible, namely in the region of $2\theta = 38^\circ$ and 40° . This shift to lower angles, of about 0.20° , indicates an important oxygen incorporation in this phase, forming the already mentioned solid solution α -Ti(N,O).

3.3. Microhardness measurements

Microhardness measurements performed on the sample surface revealed that the nitriding treatments as well as the oxidation and the combination of both lead to an increase in surface hardness compared to the initial Ti6Al4V (between 20% and 40% in nitrided samples and about 100% in the others). Anyway, these values are not representative of the oxide or nitride layers hardness. Taking into account the very low thickness of the surface layers (below 2 μm), the influence of the underlying part is highly significant. In order to overcome the difficulties in achieving more reliable values of hardness of the implanted surfaces, measurements on sample cross-sections (polished sandwich-type samples) were carried out (Fig. 3). The depth scale may not be very accurate, since it was deduced from SEM observations of the cross-sections. Taking into

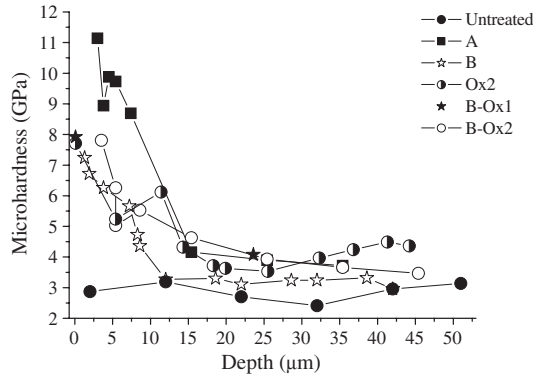


Fig. 3. Hardness measurements in cross-section of treated samples.

consideration these results and also the in-depth composition profiles (Fig. 1) and the different crystalline phases that were identified by XRD (Fig. 2), it seems reasonable to conclude that the increase of hardness is more likely related to the low concentration of nitrogen and/or oxygen incorporated in solid solution in the α -Ti phase than to the formation of different nitrides and oxide layer. Indeed, the nitrogen diffusion in α -Ti crystals is known to induce hardening of titanium alloys [11]. The hard nitride and oxide layers covering the surface are also factors to take into account for this hardness enhancement [18,19].

3.4. Tribocorrosion tests

The evolution of E_{corr} with the time is shown in Fig. 4. Several regions, identified in the graph as *a* through *d*, are present. Before placing the alumina pin in contact with the metallic surface, the samples E_{corr} was monitored for 60 min for stabilization (region *a*). After this period the potential values obtained are in the range of 0.05 to -0.05 V. During this period, two different behaviours can be observed. In samples A and B, E_{corr} increases monotonically with the immersion time, while in the others a slight decrease is observed. The stabilization of the passive film consists on the transformation of the naturally air-formed passive film into a solution-formed film. In general, an increase of the open-circuit potential with

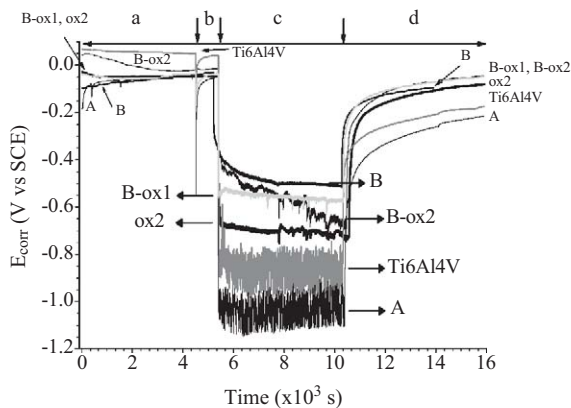


Fig. 4. Variation of the open-circuit potential (E_{corr}) for the different samples.

time is attributed to the thickening of the oxide passive layer, while a decrease of E_{corr} might be associated with breaks or partial dissolution of the passive film [20]. It is important to note that the open-circuit potential is a mixed potential reflecting both the state of the unworn disk material and that of the material in the wear track, so between those parts, a galvanic coupling may be formed (Fig. 5) [21]. The concept of active wear track area was introduced to describe the corrosion-wear process on passive materials and it corresponds to the area that loses its passive film due to a mechanical loading and also suffers from corrosion [22].

A sudden decrease of potential was observed at about 4×10^3 s. This occurs due to the contact of the alumina pin with the surface of the sample (mechanical contact), as already observed in similar systems [23,24]. In fact, when the pin is put in contact with the metallic surface, the passive film is locally destroyed, inducing the decrease of the potential. In their native form, TiO_2 films have poor tribological properties and are easily fractured under fretting and sliding wear conditions. In region *b*, the time for re-formation of the passive film can be deduced. Region *c* corresponds to the reciprocating sliding period. When sliding begins it is possible to observe an abrupt decrease of potential due to passive film removal, allowing the alloy to contact with the electrolyte.

Considering the behaviour of the untreated alloy, periodic depassivation and repassivations events in the wear scar induced by sliding are observed [25]. After a short running-in period, of about 20 min, the potential remains oscillating between -0.8 and -0.95 V vs. SCE. Nitridation at 600 °C (sample A) appears to cause a more active surface track, as the potential during sliding oscillates between ca. -0.95 and -1.1 V vs. SCE. This increase in reactivity results in a higher amount of material being removed during sliding, as it can be observed in Fig. 6, in which the weight loss measurements are plotted. According to Pons et al. [26], the wear resistance of TiN containing a low amount of N, in spite of its higher hardness, is inferior to the wear resistance of Ti (N in solid solution) due to the formation of titanium oxynitride during the sliding test. So comparing Ti6Al4V with sample A, the more active behaviour

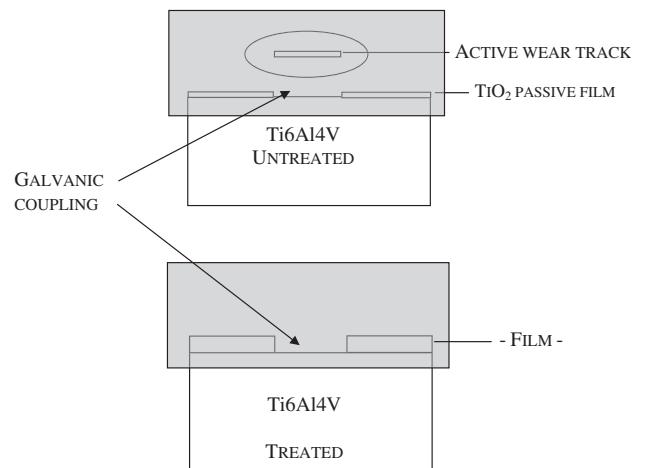


Fig. 5. Scheme of the formation of a galvanic coupling.

during the sliding of the latter could be due to the mixed potential resulting from the different chemical compositions and different crystalline phases.

However, nitridation at 700 °C (sample B) clearly decreases the thermodynamic tendency for corrosion during sliding. This enhancement of the tribocorrosion resistance might be related to the presence of the TiN crystalline phase, but more likely to the larger depth of the nitride layer ($\approx 0.25 \mu\text{m}$ for sample A and $\approx 0.7 \mu\text{m}$ for sample B, see Fig. 2). Also, the E_{corr} oscillation during sliding is significantly lower than that observed in sample nitrided at 600 °C. Nevertheless, the curve suggests that the running-in period is much larger in this sample. In fact, a stable value (ca. -500 mV vs. SCE) is obtained just after ca. 40 min of sliding. Also, as indicated in the weight loss plot (Fig. 6) this decrease in reactivity clearly results in a decrease of the amount of material removed during sliding. It should be reminded that the weight loss expressed in Fig. 6 arises from both the mechanical and the chemical/electrochemical action on the samples.

The oxidation treatment on the Ti alloy results in a slight increase of the E_{corr} , i.e. reduction in corrosion tendency. Also, as in the case of nitrided sample at 700 °C, the oscillation potential during sliding is decreased. As illustrated in Fig. 7, when a metallic material is covered by a passive film or by a coating, two different situations may occur, depending on the mechanical and physical characteristics of the film and on the mechanical solicitation at the contact region [27]. If the pin penetrates down to the metallic material (Fig. 7a), a strong dissolution (wear accelerated corrosion) is expected to occur, after the pin slides on each region. However, if the pin penetrates only slightly in the film (Fig. 7b), an increase in reactivity will occur only due to the decrease in film thickness, and it is expected to be less than in the previous situation. In any case, the wear accelerated corrosion will depend also on the rate of film re-growth, which should be lower than in case (a) [28]. It should be reminded that the structure of the samples in this work is quite more complex than that expressed in Fig. 7. In fact, the graded region under the superficial surface passive film, which consists itself of a mixture of oxides ($\text{Al}_2\text{O}_3/\text{TiO}_2$, as discussed above), is expected to have a strong influence on the tribocorrosion behaviour of the samples, and consequently the E_{corr} oscillation should be much less pronounced in this situation.

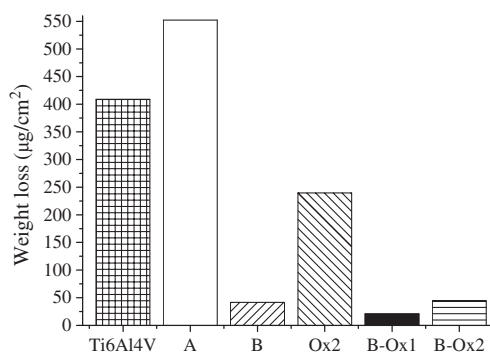


Fig. 6. Weight loss measurements.

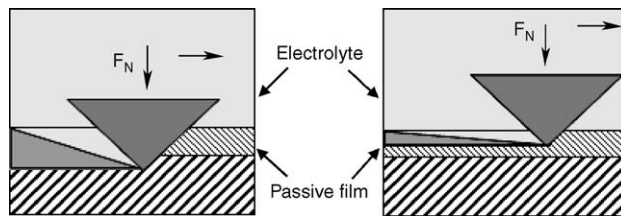


Fig. 7. Tribocorrosion model: (a) pin in contact with the substrate, (b) scratching of passive film only.

The modification of the nitride structure obtained at 700 °C by the oxidation treatment seems to degrade the electrochemical thermodynamics of the system. In fact, oxidation of the nitrided samples results in a decrease of the E_{corr} . It is interesting to note that for a longer oxidation time (sample B-ox2), the corrosion potential during sliding decreases to values approaching that of the Ti alloy oxidised sample. Nevertheless, this increase in corrosion tendency does not significantly affect the weight loss during the wear test, as shown in Fig. 6.

After sliding, the pin was raised and, as observed in region *d* in Fig. 4, repassivation of the material starts. It is possible to observe in Fig. 4, with exception of the Ti6Al4V untreated sample and the sample nitrided at 600 °C, that after repassivation the E_{corr} is similar to that measured before the test. This observation supports the fact that in the oxidised samples, and in the sample nitrided at 700 °C, the surface treated region is not completely destroyed.

EIS data is commonly analysed by fitting the experimental results (Fig. 8b) to an electrochemical equivalent circuit model. For the samples analysed in this work, the equivalent circuit model schematized in Fig. 8a was proposed, where R_{Ω} is the resistance of the electrolyte and R_p and C_p are polarization resistance and the capacitance of the film, respectively. The R_p estimated for all samples, before and after sliding, is represented in Fig. 8c. It should be referred that R_p is inversely proportional to the corrosion rate. As it can be observed in Fig. 8c, R_p after the wear test decreases in all samples, except for sample B. This decrease in R_p indicates a modification of the characteristics of the passive film formed on the surface after the wear test. In sample B, the increase of R_p is probably due to accumulation of material that enhances its resistance. It is thought that the passive oxide layer on Ti6Al4V implant alloys behaves as an efficient barrier to corrosion, and increases charge transfer resistance at the corrosion interface [29], so the untreated sample presents the highest polarization resistance, before wear tests, due to the good protective character of passive oxide layer present at the surface. However during and after sliding, this passive layer highly degrades, resulting in a decrease of both E_{corr} and R_p values (Figs. 8c and 4).

The degradation of this passive film is also confirmed by the relatively high weight loss of this sample after the wear (Fig. 6). The Ox2 sample reveals a weak polarization resistance probably justified by its “short” thermal oxidation treatment that allowed a little incorporation of oxygen into the bulk material, as detected in XRD analysis, avoiding the formation of protective “pure” oxide phases.

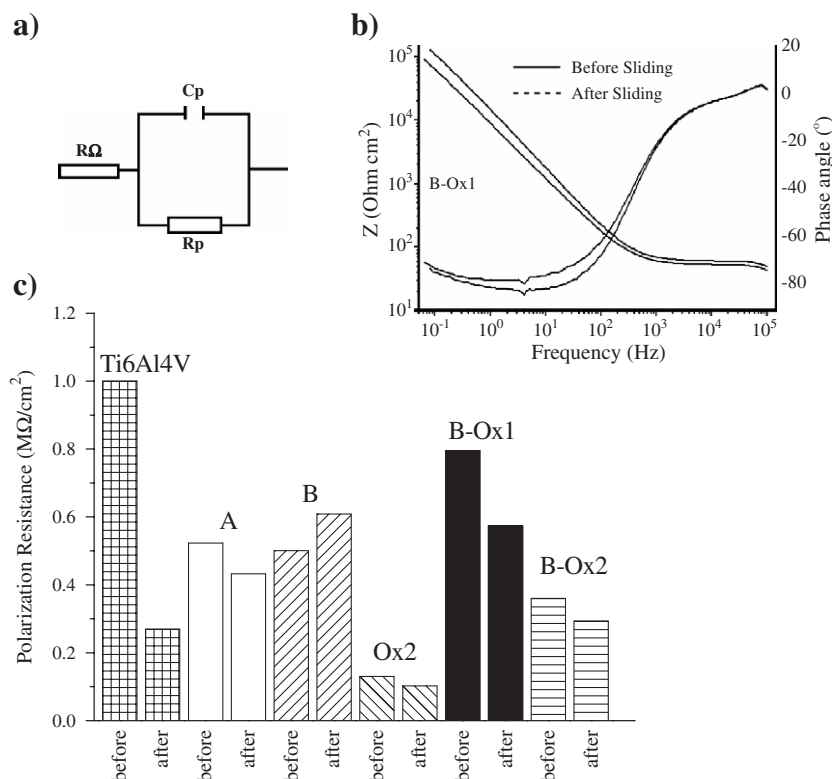


Fig. 8. (a) Equivalent circuit used for fitting the experimental data; (b) Bode plots of B-ox1 before and after the sliding; (c) polarization resistance of the passive film for both measurements (before and after sliding).

Comparing the samples A and B, it seems that the one that has been treated at higher temperature (B) has better corrosion resistance. This is in accordance with the E_{corr} and weight loss measurements obtained for these samples. Regarding the nitrided+oxidised samples (B-ox1 and B-ox2) it seems that longer oxidation time disfavours the tribocorrosion properties, as deduced from the weight loss measurements (Fig. 6) and from the R_p data (Fig. 8c). This could be related with higher oxygen incorporation that is in agreement with the Ox2 behaviour, which presents a very low R_p value. Also, as shown in Fig. 4, when sliding begins the B-ox2 presents an E_{corr} similar to B, but during sliding the E_{corr} tends to the potential of the Ox2 sample. So, it appears that O incorporation in the nitrided samples promotes the degradation of sample corrosion properties.

4. Conclusions

Nitridation leads to Ti_2N layer (almost without Al and V) of 0.25 (600 °C) and 0.7 μm (700 °C). The presence of those phases is well correlated with the chemical analysis. The nitridation does not protect from gaseous oxidation at 700 °C; the obtained oxide is more crystallised in this case compared to un-nitrided Ti6Al4V, probably because of the absence of Al in the starting nitride layer. Longer treatments should be performed to check the effective stability of this structure. All kinds of treatments resulted in hardness enhancement.

Within the used conditions, the tribocorrosion tests revealed better results in case of treatments leading to a layer thicker than 0.5 μm . The best result is obtained with the thick nitride layer

oxidised for 15 min (because it is mechanically highly resistant and chemically inert with the electrolyte solution) and it degrades for higher oxidation time. With initial Ti6Al4V or nitrided samples at 600 °C, the passive layer or the nitride layer (0.3 μm) is too thin and is completely removed during sliding, in the conditions tested in this work. The weight loss is significantly lower with the nitridation at 700 °C and for both nitrided+oxidised treatments, confirming that the nitriding treatment at 700 °C, combined with a controlled oxidation is a good solution for tribocorrosion protection.

The oxidation of Ti6Al4V leads to the lower polarisation resistance and thus a higher corrosion rate.

References

- [1] F. Berberich, W. Matz, U. Kreissig, E. Richter, N. Schell, W. Möller, Appl. Surf. Sci. 179 (2001) 13.
- [2] V. Fouquet, L. Pichon, A. Straboni, M. Drouet, Surf. Coat. Technol. 186 (2004) 34.
- [3] S. Lakshmi, D. Arivuoli, B. Ganguli, Mat. Chem. Phys. 76 (2002) 187.
- [4] V. Fouquet, L. Pichon, M. Drouet, A. Straboni, Appl. Surf. Sci. 221 (2004) 248.
- [5] S. Ma, K. Xu, W. Jie, Surf. Coat. Technol. 185 (2004) 205.
- [6] F. Berberich, W. Matz, E. Richter, N. Schell, U. KreiBig, W. Möller, Surf. Coat. Technol. 128–129 (2000) 450.
- [7] A. Fossati, F. Borgioli, E. Galvanetto, T. Bacci, Corr. Sci. 46 (2004) 917.
- [8] R. Hsu, C. Yang, C. Huang, Y. Chen, Mat. Sci. Eng. A 380 (2004) 100.
- [9] Y. Itoh, A. Itoh, H. Azuma, T. Hioki, Surf. Coat. Technol. 111 (1999) 172.
- [10] P. Pérez, Surf. Coat. Technol. 191 (2005) 293.
- [11] F. Galliano, E. Galvanetto, S. Mischler, D. Landolt, Surf. Coat. Technol. 145 (2001) 121.

- [12] R.A. Buchanan, E.D. Rigney, J.M. Williams, *J. Biomed. Mater. Res.* 21 (1987) 367.
- [13] J. Perriere, J. Siejka, N. Remili, A. Laurent, A. Straboni, B. Vuillemoz, *J. Appl. Phys.* 59 (1986) 2752.
- [14] M. Ohring, *The Materials Science of Thin Films*, Academic Press Inc., San Diego, 1992.
- [15] M. Erola, *Thin Solid Films* 156 (1988) 117.
- [16] F. Vaz, J. Ferreira, E. Ribeiro, L. Rebouta, S. Lanceros-Méndez, J.A. Mendes, F. Ribeiro, I. Moutinho, Ph. Goudeau, J.P. Rivière, E. Alves, K. Pischow, J. de Rijk, *Surf. Coat. Technol.* 191 (2005) 317.
- [17] H.L. Chu, P.K. Datta, D.B. Lewis, J.S. Burnell-Gray, *Corr. Sci.* 36 (1994) 631.
- [18] H. Güleriyüz, H. Çimenoglu, *Biomaterials* 25 (2004) 3325.
- [19] F. Borgioli, E. Galvanetto, F.P. Galliano, *Surf. Coat. Technol.* 141 (2001) 103.
- [20] A. Al-Mayouf, A. Al-Swayih, N. Al-Mobarak, A. Al-Jabab, *Mat. Chem. Phys.* 86 (2004) 320.
- [21] R. Oltra, *Wear-Corrosion Interactions in Liquid Media*, in: A.A. Sagües, E.I. Meletis (Eds.), *Minerals, Metals and Materials Soc.*, 1991, pp. 3–17.
- [22] I. García, D. Drees, J.P. Celis, *Wear* 249 (2001) 452.
- [23] S. Rossi, L. Fedrizzi, M. Leoni, P. Scardi, Y. Massiani, *Thin Solid Films* 350 (1999) 161.
- [24] T. Hara, H. Asahi, Y. Kaneta, *Corrosion* 56 (2000) 183.
- [25] S. Mischler, S. Debaud, D. Landolt, *J. Electrochem. Soc.* 145 (1998) 750.
- [26] F. Pons, J.C. Pivin, G. Farges, *J. Mater. Res.* 2 (1987) 580.
- [27] G. Zambelli, L. Vincent, *Matériaux et contacts: une approche tribologique*, Presses polytechniques et universitaires romandes Première édition, 1998.
- [28] Zhongping Yao, Zhaohua Jiang, Shigang Xin, Xuotong Sun, Xiaohong Wu, *Electrochimia*, in press.
- [29] R. Hsu, C. Yang, C. Huang, Y. Chen, *Mat. Sci. Eng. A* 380 (2004) 100.